Supporting Information

Hierarchical NiFe-hydroxide/Ni_3N nanosheet-on-nanosheet heterostructures for bifunctional oxygen evolution and urea oxidation reactions

Hongjuan Zhang,[†] *Xufeng Meng,*[†] *Jingfang Zhang*[*,†] *and Yi Huang*[‡]

[†]Department of Chemistry, College of Science, Hebei Agricultural University, Baoding 071001, China.

[‡]Key Laboratory of Pesticide & Chemical Biology of Ministry of Education, Institute of Environmental & Applied Chemistry, College of Chemistry, Central China Normal University, Wuhan 430079, China.

[*]Corresponding Author E-mail address: zjf1991211@163.com

Number of pages: 19

Number of figures: 12

Number of tables: 2

Supplementary Figures:

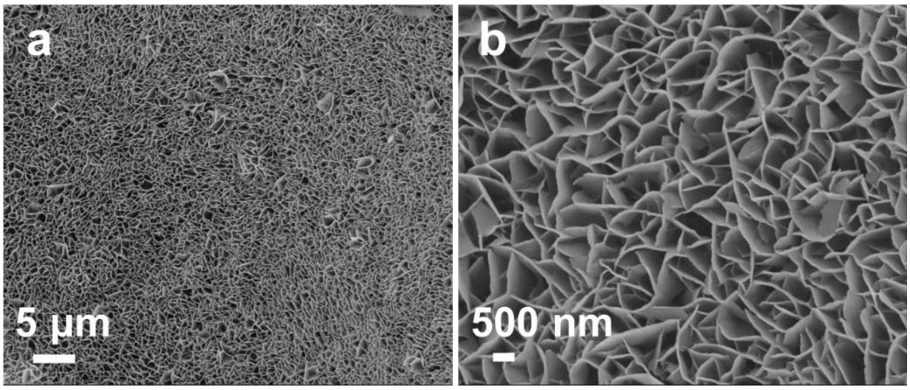

Figure S1. (a, b) SEM images of $Ni(OH)_2$ nanosheet arrays on nickel foam (NF).

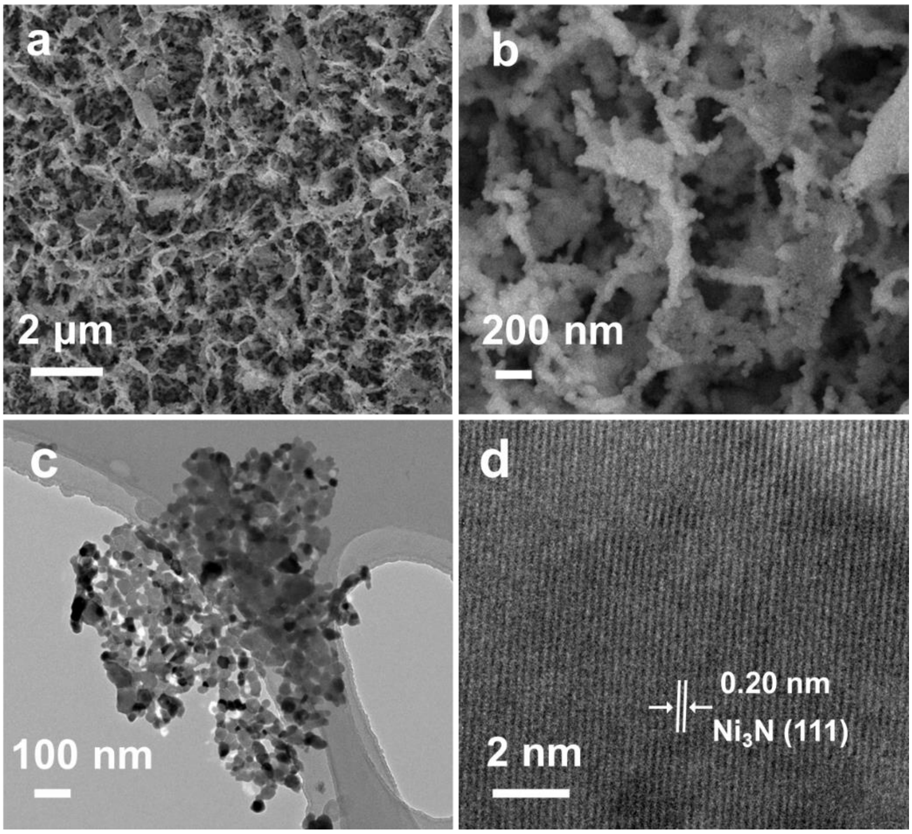

Figure S2. (a, b) SEM images, (c) TEM image and (d) HRTEM image of Ni_3N nanoparticle-assembled nanosheets.

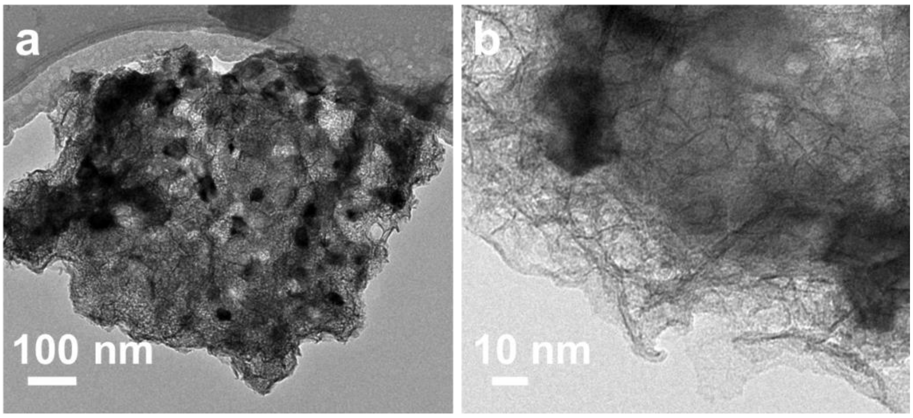

Figure S3. (a, b) TEM images of $NiFe(OH)_x/Ni_3N$.

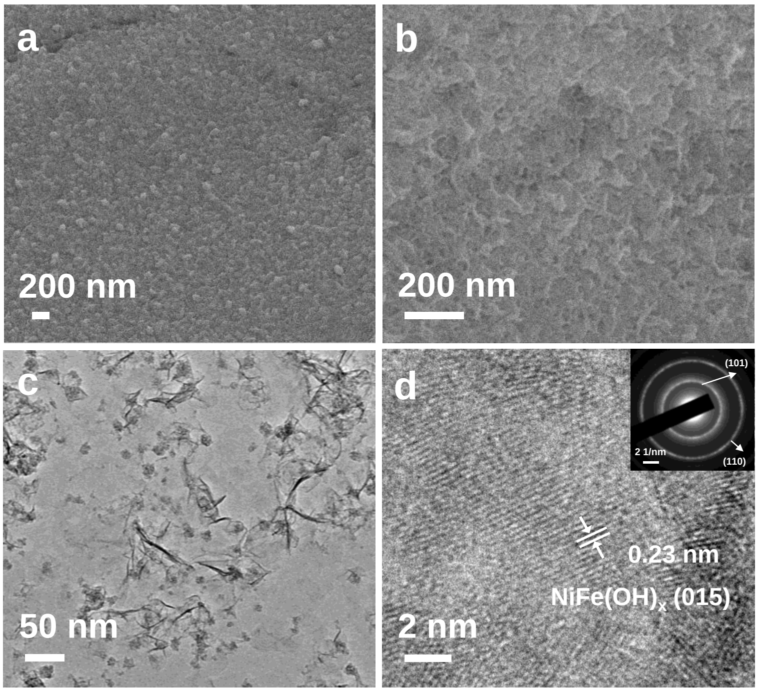

Figure S4. (a, b) SEM, (c) TEM and (d) HRTEM images of $NiFe(OH)_x$. Inset: SAED pattern of $NiFe(OH)_x$.

SEM images of $NiFe(OH)_x$ reveal the interlaced nanosheets architecture are uniformly covered on the Ni foam (Figure S4a and S4b). The nanosheet arrays could provide the enlarged active surface area and a 3D open framework for gas escaping during electrocatalysis. Furthermore, the microstructure and lattice structure of $NiFe(OH)_x$ are unveiled by TEM and HRTEM (Figures S4c and S4d). The TEM image further indicates the nanosheet morphology of $NiFe(OH)_x$. The HRTEM image of $NiFe(OH)_x$ displays the characteristic lattice fringes with distances of 0.23 nm assigned to the (015) plane of $NiFe(OH)_x$.[1] The SAED pattern displays multiple diffraction rings, indicative of polycrystalline nature of $NiFe(OH)_x$ sample. Definitely, the (101) and (110) planes of $NiFe(OH)_x$ can be well distinguished, further suggesting that the $NiFe(OH)_x$ (JCPDS card no. 40-0215) is successfully synthesized (inset of Figure S4d).

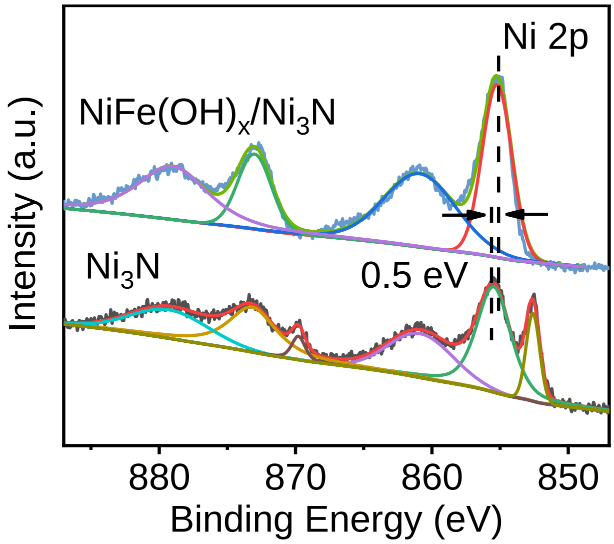

Figure S5. XPS spectra of Ni 2p for the Ni_3N and $NiFe(OH)_x/Ni_3N$.

For the Ni 2p spectrum of Ni_3N (Figure S5), the binding energies at 852.6 eV are corresponding to Ni^0, and the peaks at 855.6 and 873.4 eV are corresponding to Ni $2p_{3/2}$ and Ni $2p_{1/2}$ in Ni_3N, respectively. After electrodeposition of $NiFe(OH)_x$, the characteristic peak of Ni^0 disappears, and the peak of Ni $2p_{3/2}$ in $NiFe(OH)_x/Ni_3N$ shows a negative shift of 0.5 eV compared with pure Ni_3N, indicating the strong interfacial electronic interactions of $NiFe(OH)_x$ and Ni_3N in $NiFe(OH)_x/Ni_3N$.

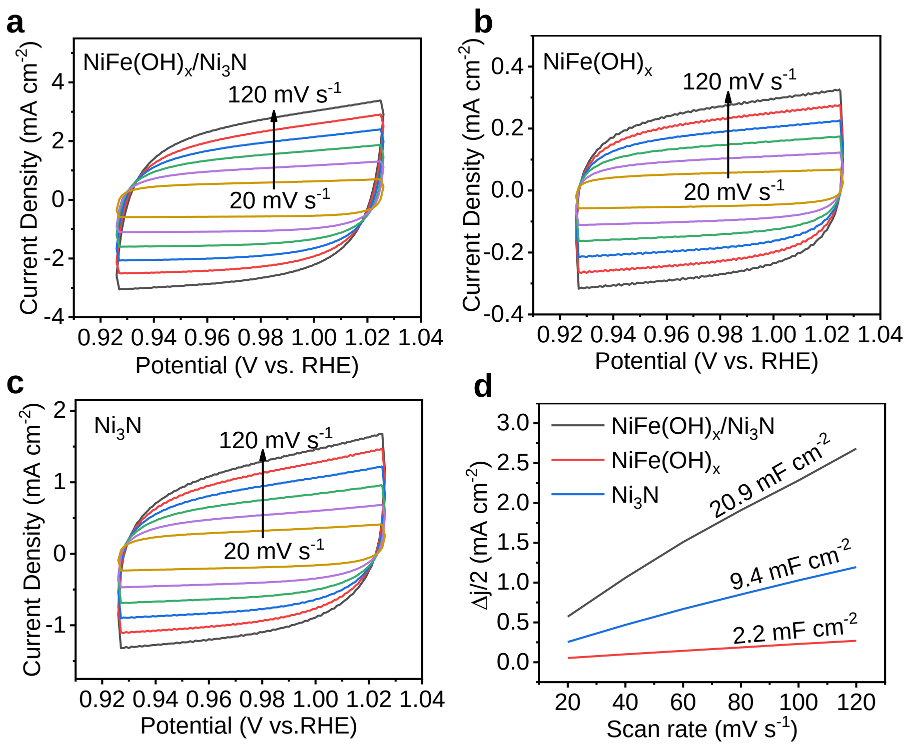

Figure S6. CV curves of (a) $NiFe(OH)_x/Ni_3N$, (b) pure $NiFe(OH)_x$, and (c) pure Ni_3N at scan rates of 20, 40, 60, 80, 100, and 120 mV s^{-1}. (d) $\Delta j/2$ of $NiFe(OH)_x/Ni_3N$, pure $NiFe(OH)_x$, and pure Ni_3N plotted versus scan rate.

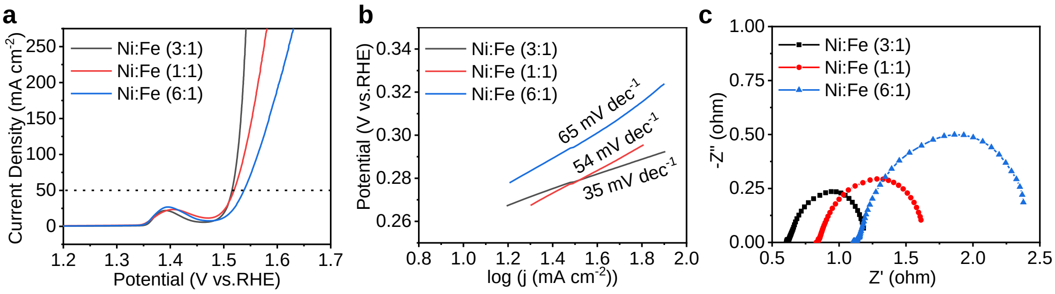

Figure S7. (a) Polarization curves, (b) Tafel plots, and (c) corresponding Nyquist plots of $NiFe(OH)_x/Ni_3N$ with different Ni : Fe molar ratios in $NiFe(OH)_x$ toward OER.

To explore the effects of Ni : Fe ratio in $NiFe(OH)_x$ on the electrocatalytic activity, $NiFe(OH)_x$ with various molar ratios of Ni : Fe were deposited on Ni_3N. Figure S7a displays the polarization curves of the Ni : Fe molar ratio of 1:1, 3:1, 6:1. The optimal molar ratio of Ni : Fe is 3:1 for OER. Therefore, in this study, the Ni : Fe ratio is 3:1 of $NiFe(OH)_x/Ni_3N$ unless otherwise noted. The Tafel slopes of $NiFe(OH)_x/Ni_3N$ with the Ni : Fe molar ratio of 1:1, 3:1 and 6:1 are 54 mV dec^{-1}, 35 mV dec^{-1} and 65 mV dec^{-1}, respectively (Figure S7b). Simultaneously, the $NiFe(OH)_x/Ni_3N$ with Ni : Fe ratio of 3:1 exhibits a smallest charge transfer resistance than that of 1:1 and 6:1, further reflecting $NiFe(OH)_x/Ni_3N$ with Ni : Fe molar ratio of 3:1 possesses a faster reaction kinetics (Figure S7c).

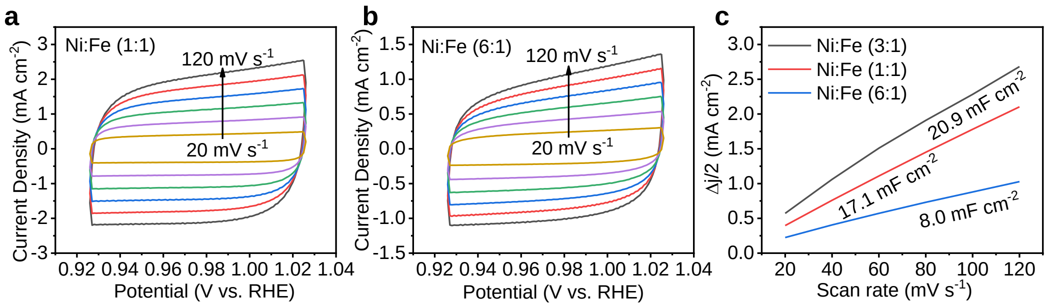

Figure S8. (a-b) CV curves of $NiFe(OH)_x/Ni_3N$ with different Ni : Fe molar ratios in $NiFe(OH)_x$ at scan rates of 20, 40, 60, 80, 100, and 120 mV s^{-1}. (c) Plots of current density versus the scan rate.

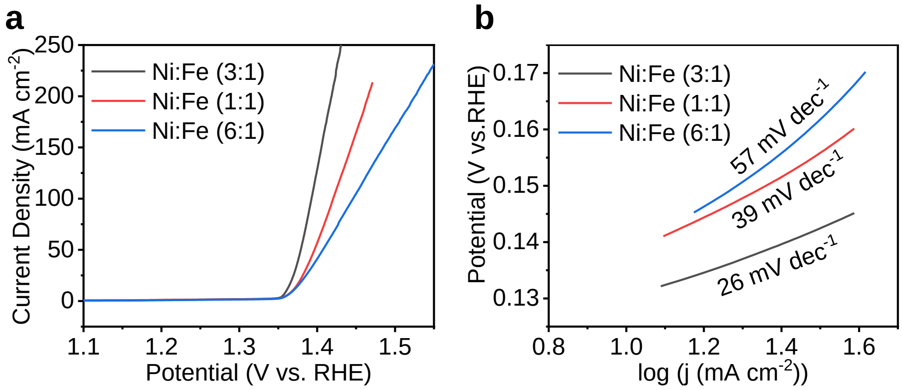

Figure S9. (a) Polarization curves, (b) corresponding Tafel plots of $NiFe(OH)_x/Ni_3N$ with different Ni : Fe molar ratios in $NiFe(OH)_x$ toward UOR.

Figure S9a displays the polarization curves for the UOR of $NiFe(OH)_x/Ni_3N$ with the Ni : Fe molar ratio of 1:1, 3:1, 6:1 in $NiFe(OH)_x$. Similar with OER, the optimal molar ratio of Ni : Fe is 3:1 for UOR. As shown in Figure S9b, Tafel slope of $NiFe(OH)_x/Ni_3N$ with the Ni : Fe molar ratio of 3:1 is calculated as 26 mV dec^{-1}, which is much smaller than that of 1:1 (39 mV dec^{-1}) and 6:1 (57 mV dec^{-1}). These results validate the $NiFe(OH)_x/Ni_3N$ with Ni : Fe molar ratio of 3:1 in $NiFe(OH)_x$ possesses the highest UOR activity.

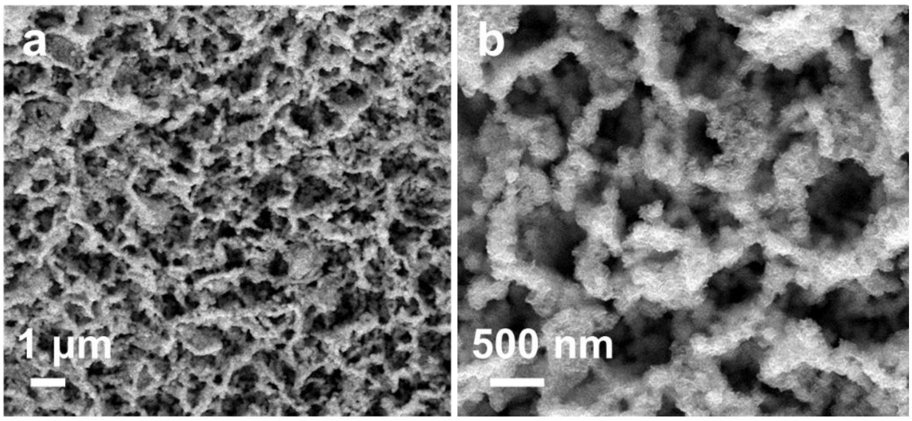

Figure S10. (a, b) SEM images of $NiFe(OH)_x/Ni_3N$ after electrocatalytic tests.

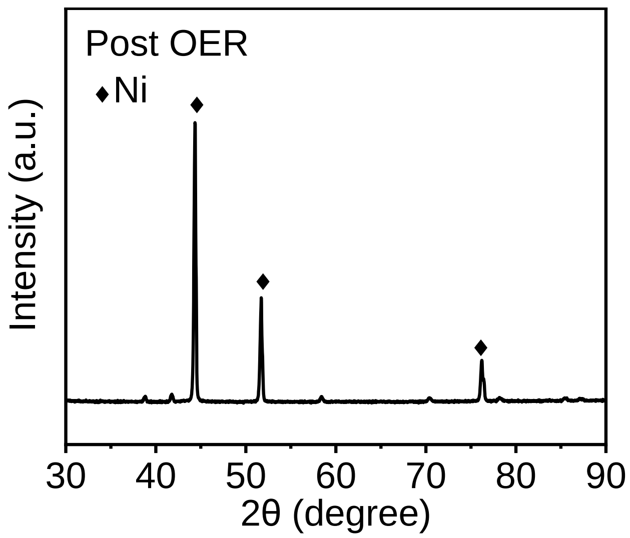

Figure S11. XRD pattern of the $NiFe(OH)_x/Ni_3N$ after electrocatalytic tests.

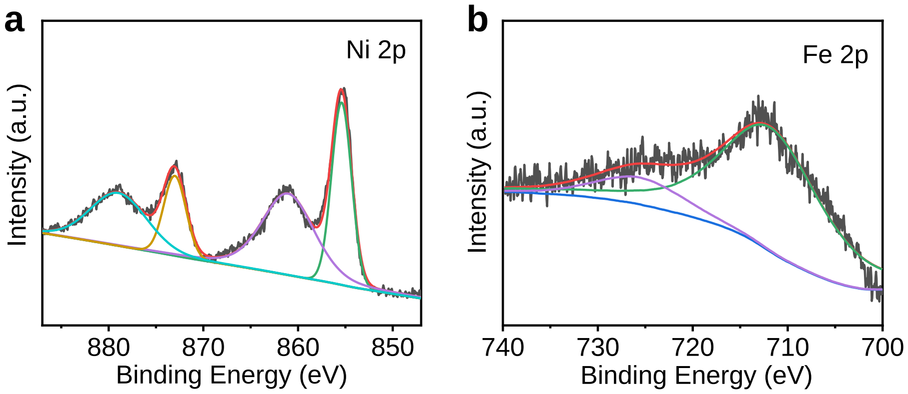

Figure S12. XPS spectra of (a) Ni 2p, and (b) Fe 2p for $NiFe(OH)_x/Ni_3N$ after electrochemical tests.

Table S1. OER performances of $NiFe(OH)_x/Ni_3N$ in this work and other reported Ni(Fe)-based electrocatalysts in 1.0 M KOH.

Materials	catalyst carrier	Mass loading (mg cm^{-2})	Electrolyte	Overpotential (mV)	Current density (mA cm^{-2})	Tafel slope (mV dec^{-1})	Reference
$NiFe(OH)_x/Ni_3N$	Ni foam	2	1.0 M KOH	260 290	10 100	35	This work
NiFe-LDH	Cu mesh	0.85	1.0 M KOH	300	100	61	2
NiO-Ni/NF	nickel foam	1.8	1.0 M KOH	323	100	101.1	3
NiO/C@NiFe-LDH	glassy carbon rotating disk	0.25	1.0 M KOH	299	10	45	4
NiFe/NiFe:Pi	carbon fiber paper	/	1.0 M KOH	290	10	38	5
$NiFe\text{-}MoO_x$ NS	glassy carbon	0.2	1.0 M KOH	276	10	56	6
Ni-Fe LDH	glassy carbon	0.16	1.0 M KOH	280	10	49.4	7
Ni_2P	FTO glass plate	0.1	1.0 M KOH	400	10	60	8
NiCoP/C	glassy carbon	/	1.0 M KOH	330	10	96	9
$(NiFe)S_2$-GN-0.2	glassy carbon	0.55	1.0 M KOH	320	10	61	10

NiCo LDH	carbon paper	0.17	1.0 M KOH	367	10	40	11
$NaBH_4$–NiFe LDH	Ni foam	/	1.0 M KOH	280	10	56	12
Ni MOF	carbon paper	0.48	1.0 M KOH	346	10	64	13
CoNiMn-LDH/PPy/RGO	glassy carbon	0.2	1.0 M KOH	369	10	77	14
Ni_3FeN/r-GO-20	Ni foam	0.5	1.0 M KOH	270	10	54	15
NiFe-LDH/Co,N-CNF	glassy carbon	0.12	0.1 m KOH	312	10	60	16
NiO/Ni	graphite	0.5	1.0 M KOH	345	10	53	17

Table S2. UOR performances of $NiFe(OH)_x/Ni_3N$ in this work and other reported Ni(Fe)-based electrocatalysts.

Materials	Potential (V)	Current density (mA cm^{-2})	Tafel slope (mV dec^{-1})	Reference
$NiFe(OH)_x/Ni_3N$	1.36 1.39	10 100	26	This work
pa-NiFe LDH NS/NIF	1.459	100	33	18
$Fe-Ni_3S_2@FeNi_3-8$	1.40	10	29	19
NF/NiMoO-Ar	1.42	100	19	20
Ni_3N/NF	1.4	100	41	21
Ni_2P/CFC	1.42	10	78.2	22

References:

(1) Zhang, H.; Li, X.; Hähnel, A.; Naumann, V.; Lin, C.; Azimi, S.; Schweizer, S. L.; Maijenburg, A. W.; Wehrspohn, R. B., Bifunctional Heterostructure Assembly of NiFe LDH Nanosheets on NiCoP Nanowires for Highly Efficient and Stable Overall Water Splitting. *Adv. Funct. Mater.* **2018**, *28*, 1706847.

(2) Wang, H.; Zhou, T.; Li, P.; Cao, Z.; Xi, W.; Zhao, Y.; Ding, Y., Self-Supported Hierarchical Nanostructured NiFe-LDH and Cu_3P Weaving Mesh Electrodes for Efficient Water Splitting. *ACS Sustainable Chem. Eng.* **2017**, *6*, 380-388.

(3) Yue, Z.; Zhu, W.; Li, Y.; Wei, Z.; Hu, N.; Suo, Y.; Wang, J., Surface Engineering of a Nickel Oxide–Nickel Hybrid Nanoarray as a Versatile Catalyst for Both Superior Water and Urea Oxidation. *Inorg. Chem.* **2018**, *57*, 4693-4698.

(4) Li, X.; Fan, M.; Wei, D.; Wang, X.; Wang, Y., Core-Shell NiO/C@NiFe-LDH Nanocomposite as an Efficient Electrocatalyst for Oxygen Evolution Reaction. *J. Electrochem. Soc.* **2020**, *167*, 024501.

(5) Li, Y.; Zhao, C., Enhancing Water Oxidation Catalysis on a Synergistic Phosphorylated NiFe Hydroxide by Adjusting Catalyst Wettability. *ACS Catal.* **2017**, *7*, 2535-2541.

(6) Xie, C.; Wang, Y.; Hu, K.; Tao, L.; Huang, X.; Huo, J.; Wang, S., In Situ Confined Synthesis of Molybdenum Oxide Decorated Nickel-Iron Alloy Nanosheets from MoO_4^{2-} Intercalated Layered Double Hydroxides for the Oxygen Evolution Reaction. *J. Mater. Chem. A* **2017**, *5*, 87-91.

(7) Yu, L.; Yang, J. F.; Guan, B. Y.; Lu, Y.; Lou, X. W., Hierarchical Hollow Nanoprisms Based on Ultrathin Ni-Fe Layered Double Hydroxide Nanosheets with Enhanced Electrocatalytic Activity towards Oxygen Evolution. *Angew. Chem. Int. Ed.* **2018**, *57*, 172-176.

(8) Han, A.; Chen, H.; Sun, Z.; Xu, J.; Du, P., High Catalytic Activity for Water Oxidation Based on Nanostructured Nickel Phosphide Precursors. *Chem. Commun.* **2015**, *51*, 11626-11629.

(9) He, P.; Yu, X.-Y.; Lou, X. W., Carbon-Incorporated Nickel-Cobalt Mixed Metal Phosphide Nanoboxes with Enhanced Electrocatalytic Activity for Oxygen Evolution. *Angew. Chem. Int. Ed.* **2017**, *56*, 3897-3900.

(10) Liu, C.; Ma, H.; Yuan, M.; Yu, Z.; Li, J.; Shi, K.; Liang, Z.; Yang, Y.; Zhu, T.; Sun, G.; Li, H.; Ma, S., $(NiFe)S_2$ Nanoparticles Grown on Graphene as an Efficient Electrocatalyst for Oxygen Evolution Reaction. *Electrochim. Acta* **2018**, *286*, 195-204.

(11) Liang, H.; Meng, F.; Caban-Acevedo, M.; Li, L.; Forticaux, A.; Xiu, L.; Wang, Z.; Jin, S., Hydrothermal Continuous Flow Synthesis and Exfoliation of NiCo Layered Double Hydroxide Nanosheets for Enhanced Oxygen Evolution Catalysis. *Nano Lett.* **2015**, *15*, 1421-1427.

(12) Wang, Y.; Tao, S.; Lin, H.; Han, S.; Zhong, W.; Xie, Y.; Hu, J.; Yang, S., $NaBH_4$ Induces a High Ratio of Ni^{3+}/Ni^{2+} Boosting OER Activity of the NiFe LDH Electrocatalyst. *RSC Adv.* **2020**, *10*, 33475-33482.

(13) Maruthapandian, V.; Kumaraguru, S.; Mohan, S.; Saraswathy, V.; Muralidharan, S., An Insight on the Electrocatalytic Mechanistic Study of Pristine Ni

MOF (BTC) in Alkaline Medium for Enhanced OER and UOR. *ChemElectroChem* **2018**, *5*, 2795-2807.

(14) Jia, X.; Gao, S.; Liu, T.; Li, D.; Tang, P.; Feng, Y., Fabrication and Bifunctional Electrocatalytic Performance of Ternary CoNiMn Layered Double Hydroxides/Polypyrrole/Reduced Graphene Oxide Composite for Oxygen Reduction and Evolution Reactions. *Electrochim. Acta* **2017**, *245*, 51-60.

(15) Gu, Y.; Chen, S.; Ren, J.; Jia, Y. A.; Chen, C.; Komarneni, S.; Yang, D.; Yao, X., Electronic Structure Tuning in Ni_3FeN/r-GO Aerogel toward Bifunctional Electrocatalyst for Overall Water Splitting. *ACS Nano* **2018**, *12*, 245-253.

(16) Wang, Q.; Shang, L.; Shi, R.; Zhang, X.; Zhao, Y.; Waterhouse, G. I. N.; Wu, L.-Z.; Tung, C.-H.; Zhang, T., NiFe Layered Double Hydroxide Nanoparticles on Co,N-Codoped Carbon Nanoframes as Efficient Bifunctional Catalysts for Rechargeable Zinc-Air Batteries. *Adv. Energy Mater.* **2017**, *7*, 1700467.

(17) Liang, J.; Wang, Y.-Z.; Wang, C.-C.; Lu, S.-Y., In Situ Formation of NiO on Ni Foam Prepared with a Novel Leaven Dough Method as an Outstanding Electrocatalyst for Oxygen Evolution Reactions. *J. Mater. Chem. A* **2016**, *4*, 9797-9806.

(18) Xie, J.; Qu, H.; Lei, F.; Peng, X.; Liu, W.; Gao, L.; Hao, P.; Cui, G.; Tang, B., Partially Amorphous Nickel-Iron Layered Double Hydroxide Nanosheet Arrays for Robust Bifunctional Electrocatalysis. *J. Mater. Chem. A* **2018**, *6*, 16121-16129.

(19) Zhang, W.; Jia, Q.; Liang, H.; Cui, L.; Wei, D.; Liu, J., Iron Doped Ni_3S_2 Nanorods Directly Grown on $FeNi_3$ Foam as an Efficient Bifunctional Catalyst for Overall Water Splitting. *Chem. Eng. J.* **2020**, *396*, 125315.

(20) Yu, Z.-Y.; Lang, C.-C.; Gao, M.-R.; Chen, Y.; Fu, Q.-Q.; Duan, Y.; Yu, S.-H., Ni-Mo-O Nanorod-Derived Composite Catalysts for Efficient Alkaline Water-to-Hydrogen Conversion via Urea Electrolysis. *Energy Environ. Sci.* **2018**, *11*, 1890-1897.

(21) Hu, S.; Feng, C.; Wang, S.; Liu, J.; Wu, H.; Zhang, L.; Zhang, J., Ni_3N/NF as Bifunctional Catalysts for Both Hydrogen Generation and Urea Decomposition. *ACS Appl. Mater. Interfaces* **2019**, *11*, 13168-13175.

(22) Zhang, X.; Liu, Y.; Xiong, Q.; Liu, G.; Zhao, C.; Wang, G.; Zhang, Y.; Zhang, H.; Zhao, H., Vapour-Phase Hydrothermal Synthesis of Ni_2P Nanocrystallines on Carbon Fiber Cloth for High-Efficiency H_2 Production and Simultaneous Urea Decomposition. *Electrochim. Acta* **2017**, *254*, 44-49.